HHS Public Access

Author manuscript

Cell Rep. Author manuscript; available in PMC 2017 October 27.

Published in final edited form as:

Cell Rep. 2017 September 19; 20(12): 2775–2783. doi:10.1016/j.celrep.2017.08.025.

A protein scaffold coordinates SRC-mediated JNK activation in response to metabolic stress

Shashi Kant[1,2,†,¶], **Claire L. Standen**[1,†], **Caroline Morel**[1,†], **Dae Young Jung**[1], **Jason K. Kim**[1,3], **Wojciech Swat**[4], **Richard A. Flavell**[5], and **Roger J. Davis**[1,6,¶,*]

[1]Program in Molecular Medicine, University of Massachusetts Medical School, Worcester, Massachusetts 01605, USA

[2]Division of Cardiovascular Medicine, Department of Medicine, University of Massachusetts Medical School, Worcester, Massachusetts 01605, USA

[3]Division of Endocrinology, Metabolism and Diabetes, Department of Medicine, University of Massachusetts Medical School, Worcester, Massachusetts 01605, USA

[4]Department of Pathology and Immunology, Washington University School of Medicine, St. Louis, Missouri 63110, USA

[5]Howard Hughes Medical Institute and Department of Immunobiology, Yale University School of Medicine, New Haven, Connecticut 06520, USA

[6]Howard Hughes Medical Institute, Worcester, Massachusetts 01605, USA

SUMMARY

Obesity is a major risk factor for the development of metabolic syndrome and type 2 diabetes. How obesity contributes to metabolic syndrome is unclear. Free fatty acid (FFA) activation of a non-receptor tyrosine kinase (SRC)-dependent cJun NH_2-terminal kinase (JNK) signaling pathway is implicated in this process. However, the mechanism that mediates SRC-dependent JNK activation is unclear. Here we identify a role for the scaffold protein JIP1 in SRC-dependent JNK activation. SRC phosphorylation of JIP1 creates phosphotyrosine interaction motifs that bind the SH2 domains of SRC and the guanine nucleotide exchange factor VAV. These interactions are required for SRC-induced activation of VAV and the subsequent engagement of a JIP1-tethered JNK signaling module. The JIP1 scaffold protein therefore plays a dual role in FFA signaling by

[¶]Corresponding authors: Shashi.Kant@umassmed.edu and Roger.Davis@umassmed.edu.
[†]Equal contributions.
[*]Lead Contact: Roger.Davis@umassmed.edu

SUPPLEMENTAL INFORMATION

Supplemental Information includes four figures and experimental procedures.

AUTHOR CONTRIBUTIONS

S.K., C.M., C.S., W.S., J.K.K., R.A.F. and R.J.D. designed research. S.K., C.M., C.S. and D.Y.J. performed research. S.K., C.M., C.S., J.K.K. and R.J.D. analyzed the data. S.K. and R.J.D. wrote the manuscript.

coordinating upstream SRC functions together with down-stream effector signaling by the JNK pathway.

Graphical abstract

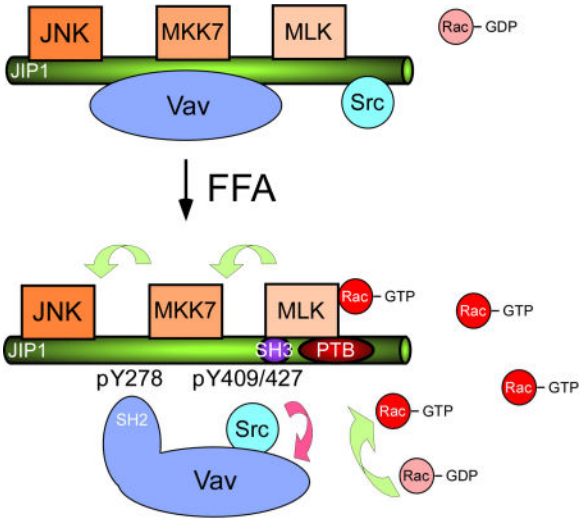

INTRODUCTION

Human obesity is a worldwide health problem that is associated with metabolic syndrome and the development of insulin resistance and type 2 diabetes (Flegal et al., 2013). Effects of obesity on metabolic syndrome are mediated, in part, by increased amounts of saturated free fatty acid (FFA) in the blood (Kahn et al., 2006). A key signaling mechanism that is activated by FFA is the cJun NH_2-terminal kinase (JNK) stress response pathway (Davis, 1994, 2000). Studies using JNK-deficient mice demonstrate that JNK signaling is required for the development of obesity and insulin resistance (Sabio and Davis, 2010). Consequently, components of the JNK signaling pathway represent potential targets for the design of drugs that may be useful for the treatment of metabolic syndrome (Sabio and Davis, 2010).

The mechanism of JNK activation caused by FFA is unclear. Recent studies have identified the non-receptor tyrosine kinase SRC (Holzer et al., 2011), the small GTPase RAC1 (Sharma et al., 2012), and the mixed-lineage protein kinase (MLK) family of MAP3K (Craige et al., 2016; Jaeschke and Davis, 2007; Kant et al., 2013; Sharma et al., 2012) as components of a FFA-stimulated signaling pathway that activates JNK. However, the mechanism that mediates signaling has not been established. Here we report that the scaffold protein JIP1 can serve to link SRC, RAC1, and MLK in a FFA-stimulated signaling pathway.

RESULTS

JIP1 is required for FFA-stimulated SRC activation and redistribution to lipid rafts

The scaffold protein JIP1 binds SRC family members (Kennedy et al., 2007; Nihalani et al., 2007) and is implicated in the MLK pathway that leads to JNK activation (Jaeschke et al., 2004; Morel et al., 2010; Whitmarsh et al., 1998; Whitmarsh et al., 2001). It is established that FFA causes SRC redistribution to Triton-insoluble lipid rafts (Holzer et al., 2011). To test whether JIP1 might contribute to SRC function, we examined whether FFA-treatment caused a similar redistribution of JIP1. This analysis demonstrated increased amounts of JIP1, SRC, and activated pY^{416}-SRC in the Triton insoluble fraction of cells exposed to FFA (Figure 1A). Moreover, immunofluorescence analysis of Triton-permeabilized cells demonstrated co-localization of JIP1 and SRC in FFA-treated cells (Figure 1B).

The co-regulation of SRC and JIP1 (Figure 1A,B) indicated that JIP1 may contribute to FFA signaling. We therefore compared the response of wild-type (WT) and *Jip1*$^{-/-}$ cells to FFA. Treatment of WT primary murine embryo fibroblasts (MEF) with FFA caused JNK activation and the redistribution of SRC and activated pY^{416}-SRC to lipid rafts (Figure 1C,D). In contrast, *Jip1*$^{-/-}$ MEF were resistant to FFA-stimulated JNK activation and SRC redistribution to Triton-insoluble lipid rafts. Together, these data demonstrate that JIP1 is required for the regulation of both SRC and JNK by FFA.

The requirement of JIP1 for FFA-stimulated JNK activation (Figure 1C) may represent a general role of JIP1 in JNK signaling. We therefore compared JNK activation in WT and *Jip1*$^{-/-}$ MEF in response to the inflammatory cytokine tumor necrosis factor α (TNFα). This analysis demonstrated that TNFα causes similar JNK activation in control and JIP1-deficient cells (Figure S1). JIP1 therefore plays a selective role in JNK activation, including FFA signaling.

The JIP1 JNK binding domain is required for HFD-induced insulin resistance

To test whether JIP1-mediated JNK activation is relevant to the metabolic stress response *in vivo*, we established mice lacking the JNK binding domain of JIP1 ($JIP1^{\Delta JBD}$ mice). The core of the JNK binding domain (Leu^{160}-Asn^{161}-Leu^{162}) binds a hydrophobic pocket on JNK (Heo et al., 2004; Whitmarsh et al., 1998) and is required for JIP1-mediated JNK activation (Whitmarsh et al., 1998). This core motif was replaced with Gly^{160}-Arg^{161}-Gly^{162} in $JIP1^{\Delta JBD}$ mice (Figure S2). Control studies demonstrated that MEF derived from $JIP1^{\Delta JBD}$ mice were resistant to FFA-stimulated JNK activation (Figure 2A). Comparison of WT and $JIP1^{\Delta JBD}$ mice fed a chow diet (ND) or a high fat diet (HFD) demonstrated that the HFD-induced insulin intolerance detected in WT mice was suppressed in $JIP1^{\Delta JBD}$ mice (Figure 2B). The improved insulin tolerance of HFD-fed $JIP1^{\Delta JBD}$ mice was associated with markedly decreased HFD-induced hyperinsulinemia compared with WT mice (Figure 2C).

Hyperinsulinemic-euglycemic clamp analysis of glucose infusion rates confirmed that HFD-fed $JIP1^{\Delta JBD}$ mice were more insulin sensitive than HFD-fed WT mice (Figure 2D). Moreover, the HFD-fed $JIP1^{\Delta JBD}$ mice exhibited decreased hepatic glucose production (Figure 2E), increased hepatic insulin action (Figure 2F), and increased whole body glucose turnover (Figure 2G) compared with HFD-fed WT mice. These phenotypes were associated

with increased energy expenditure and decreased obesity (Figure S3), reduced adipose tissue hypertrophy (Figure S4A,B), and reduced hepatic steatosis (Figure S4C). This protection of HFD-fed JIP1$^{\Delta JBD}$ mice against obesity and insulin resistance is similar to that detected in JNK-deficient mice (Sabio and Davis, 2010). Together, these data establish that JIP1-mediated JNK activation contributes to the HFD-induced metabolic stress response *in vivo*.

VAV, RAC1, MLK, and MKK7 contribute to JIP1-mediated JNK activation

To examine the mechanism of JIP1-mediated JNK activation caused by exposure of cells to saturated FFA, we tested the role of JNK pathway components that interact with JIP1, including the MAP2K isoform MKK7 and the mixed-lineage protein kinase (MLK) family of MAP3K (Whitmarsh et al., 1998). Analysis of WT and *Mkk7*$^{-/-}$ MEF demonstrated that MKK7 is required for FFA-stimulated JNK activation (Figure 3A). To test the role of the MLK group of MAP3K, we examined the effect of dual deficiency of MLK2 plus MLK3, the major MLK family members expressed by MEF (Kant et al., 2011). Comparison of WT and *Mlk2*$^{-/-}$ *Mlk3*$^{-/-}$ MEF demonstrated that MLK protein kinases are essential for FFA-stimulated JNK activation (Figure 3B). In contrast, we found that MLK protein kinases were not required for FFA-stimulated SRC and activated SRC redistribution to lipid rafts (Figure 3C). This analysis identifies SRC as an upstream component of the JIP1-mediated MLK-MKK7-JNK signaling pathway that is activated by FFA.

MLK isoforms can be activated by the RHO family GTPase RAC1 by binding to a conserved MLK CRIB domain (Teramoto et al., 1996). To test whether this CRIB-mediated mechanism contributes to FFA-stimulated JNK activation, we examined the effect of an inactivating mutation in the MLK3 CRIB domain (Ile^{492} Ser^{493} replaced with Ala^{492} Ala^{493}) in the context of deficiency of the redundant isoform MLK2 (Kant et al., 2011). Comparison of WT and *Mlk2*$^{-/-}$ *Mlk3*$^{\Delta CRIB/\Delta CRIB}$ MEF demonstrated that the MLK CRIB domain is essential for FFA-stimulated JNK activation (Figure 3D). This mechanism is consistent with the observation that RAC1 activation is required for the regulation of JNK activity by FFA (Sharma et al., 2012).

The exchange factor VAV has been implicated in JNK activation (Crespo et al., 1996; Kant et al., 2011). To test whether VAV contributes to FFA-stimulated JNK activation, we compared JNK activity in WT and VAV-deficient (*Vav1*$^{-/-}$ *Vav2*$^{-/-}$ *Vav3*$^{-/-}$) cells. This analysis demonstrated that VAV is required for FFA-stimulated JNK activation (Figure 3E). Moreover, FFA-treatment caused an interaction between VAV and JIP1 that was detected by co-immunoprecipitation analysis (Figure 3F). FFA-treatment also caused JIP1-dependent redistribution of VAV to lipid rafts (Figure 3G), although VAV was not required for the lipid raft association of JIP1 (Figure 3H).

FFA causes SRC-mediated tyrosine phosphorylation of JIP1 and VAV

The interaction between VAV and JIP1 was associated with FFA-stimulated tyrosine phosphorylation of both proteins (Figure 3F). The role of JIP1 tyrosine phosphorylation is unclear, but it is established that tyrosine phosphorylation of VAV increases GTP/GDP exchange activity on RAC1 (Crespo et al., 1997). To examine the mechanism of FFA-stimulated tyrosine phosphorylation of JIP1 and VAV, we tested the potential role of SRC

family tyrosine kinases. These studies were performed using *Src*$^{-/-}$ *Fyn*$^{-/-}$ *Yes*$^{-/-}$ (SFY) cells. Treatment of SFY cells with FFA did not cause JNK activation (Figure 3I) or tyrosine phosphorylation of JIP1 and VAV (Figure 3J). In contrast, complementation analysis demonstrated that the expression of SRC restored both JNK activation and tyrosine phosphorylation of both JIP1 and VAV in FFA-treated cells (Figure 3I,J). Furthermore, SRC was required for JIP1 redistribution to lipid rafts (Figure 3K). SRC family protein kinases therefore function as components of the JNK signaling pathway activated by treatment of cells with FFA.

To test whether SRC-mediated activation of JNK is mediated by the MLK pathway, we expressed constitutively activated SRC (SRC^{Y529F}) in WT and *Mlk2*$^{-/-}$ *Mlk3*$^{-/-}$ MEF. Activated SRC caused JNK activation selectively in the WT MEF (Figure 3L). These data demonstrate that the MLK pathway is an essential mediator of SRC-induced JNK activation.

Previous studies of JIP1 tyrosine phosphorylation have implicated roles for both ABL (Dajas-Bailador et al., 2008) and SRC (Kennedy et al., 2007; Nihalani et al., 2007). To confirm the role of SRC in FFA-stimulated tyrosine phosphorylation of JIP1, we examined the effect of drugs that selectively inhibit ABL and SRC. This analysis demonstrated that the SRC-selective inhibitor AZD0530, but not the ABL-selective inhibitor Gleevec, prevented FFA-stimulated tyrosine phosphorylation of JIP1 (Figure 4A). These data confirm that SRC family tyrosine kinases contribute to FFA-stimulated tyrosine phosphorylation of JIP1 (Figure 4A).

Tyrosine phosphorylation of JIP1 is required for FFA-stimulated JNK activation

JIP1 is extensively phosphorylated (D'Ambrosio et al., 2006), including on sites of tyrosine (Y^{278}, Y^{409} and Y^{427}) phosphorylation (Dajas-Bailador et al., 2008; Kennedy et al., 2007; Nihalani et al., 2007). This phosphorylation may create sites of interaction for signaling proteins with SH2 domains. Indeed, phosphotyrosine-dependent binding of JIP1 to the SH2 domain of SRC family proteins has been identified (Kennedy et al., 2007; Nihalani et al., 2007). A similar interaction might account for the binding of JIP1 to VAV. To test SH2 domain binding to JIP1, we examined the interaction of JIP1 with the SH2 domains of SRC and VAV2. This analysis demonstrated that JIP1 from FFA-treated cells bound to SRC-SH2 and VAV2-SH2 (Figure 4B,C). In contrast, JIP1 from control cells did not bind VAV2-SH2, but a low level of interaction with SRC-SH2 was detected (Figure 4B,C).

To examine the role of JIP1 tyrosine phosphorylation in JNK activation caused by saturated FFA, we performed complementation analysis using *Jip1*$^{-/-}$ MEF expressing WT or mutated JIP1 proteins. Two sites of tyrosine phosphorylation on JIP1 (pY^{409}DNC and pY^{427}EEA) are similar to the optimal sequence (pYEEI) for phosphotyrosine binding by the SRC-SH2 domain (Songyang et al., 1993). Mutational analysis indicated that Y^{409} and Y^{427} serve partially redundant functions. We therefore examined the function of JIP1 with dual mutation at Y^{409} plus Y^{427}. This analysis demonstrated that tyrosine phosphorylation of JIP1 was increased when cells were treated with FFA (Figure 4D). In contrast, phosphotyrosine was not detected on the mutated JIP1$^{Y409/427F}$ protein (Figure 4D). Co-immunoprecipitation analysis demonstrated that the interaction of SRC with JIP1 in control and FFA-treated cells was suppressed in studies with the mutated JIP1$^{Y409/427F}$ protein

(Figure 4D). Furthermore, the FFA-stimulated redistribution of JIP1 and SRC to lipid rafts depends on these sites of JIP1 tyrosine phosphorylation (Figure 4E). These data indicate that Y^{409} and Y^{427} are required for FFA-stimulated JIP1 tyrosine phosphorylation and SRC binding.

One site of tyrosine phosphorylation on JIP1 (pY^{278}LTP) is similar to the optimal sequence (pYMEP) for phosphotyrosine binding by the VAV SH2 domain (Songyang et al., 1994). Comparison of *Jip1*$^{-/-}$ MEF expressing WT and JIP1^{Y278F} proteins demonstrated that treatment with FFA promoted the co-immunoprecipitation of VAV with JIP1 and that this interaction was dependent on Y^{278} (Figure 4F). The phosphorylation site Y^{278} is therefore required for the FFA-induced interaction of JIP1 and VAV.

To test the requirement of JIP1 tyrosine phosphorylation for FFA-stimulated JNK activation, we compared *Jip1*$^{-/-}$ MEF expressing WT JIP1 and mutated JIP proteins (JIP1^{Y278F} or JIP1$^{Y409/427F}$). This analysis demonstrated that expression of WT JIP1 in *Jip1*$^{-/-}$ MEF restored FFA-stimulated JNK activation (Figure 4G). In contrast, FFA-stimulated JNK activation was not detected in *Jip1*$^{-/-}$ MEF expressing JIP1^{Y278F} or JIP1$^{Y409/427F}$ (Figure 4G). Together, these data indicate that the tyrosine phosphorylation-dependent interaction of JIP1 with SRC and VAV is required for FFA-stimulated JNK activation (Figure 4H).

DISCUSSION

An understanding of the physiological mechanism of FFA-stimulated JNK activation has remained elusive because several potential pathways have been implicated. Indeed, it is likely that FFA-stimulated JNK activation may occur by more than one mechanism *in vivo*, possibly in a cell-type and context specific manner. These potential mechanisms include: 1) the FFA-induced endoplasmic reticulum unfolded protein response (Fu et al., 2012); 2) FFA ligand binding to G protein coupled receptors (Alvarez-Curto and Milligan, 2016; Moran et al., 2016); 3) FFA metabolism and accumulation of signaling lipids, including diacylglycerol, ceramide, and sphingosine-1-phosphate (Hu et al., 2009; Montell et al., 2001; Schmitz-Peiffer et al., 1999); 4) FFA-stimulated NBR1-MEKK3 signaling (Hernandez et al., 2014); and 5) FFA-stimulated lipid raft signaling (Holzer et al., 2011). It is also possible that FFA causes JNK activation as part of a generalized lipotoxic stress response (Neuschwander-Tetri, 2010).

Here we examined the lipid raft signaling mechanism of FFA-stimulated JNK activation (Holzer et al., 2011). Previous studies have demonstrated roles for SRC (Holzer et al., 2011), RAC1 (Sharma et al., 2012), and the MLK group of MAP3K (Jaeschke and Davis, 2007; Kant et al., 2013). While VAV can load GTP on RAC1 and activate MLK (Teramoto et al., 1996), the role of SRC in this signaling pathway has not been established (Holzer et al., 2011).

Our analysis demonstrates that the scaffold protein JIP1 plays a dual role in FFA signaling by co-ordinating upstream SRC functions together with down-stream effector signaling by the JNK pathway (Figure 4H). SRC phosphorylation of JIP1 creates phosphotyrosine interaction motifs that bind the SH2 domains of SRC and the guanine nucleotide exchange

factor VAV. These interactions are required for SRC-induced tyrosine phosphorylation and activation of VAV and the subsequent engagement of a JIP1-tethered JNK signaling module (Figure 4H). It is likely that this mechanism contributes to physiological regulation because defects in JIP1 (Jaeschke et al., 2004; Morel et al., 2010), including disruption of the JIP1 JNK binding site (Figure 2), strongly suppress the consequences of HFD consumption by mice.

The interaction of JIP1 with signaling molecules provides an opportunity for the design of small molecules to disrupt FFA-stimulated JNK activation. This approach has been employed to identify drugs that target the JNK/JIP1 interaction (Chen et al., 2009; Stebbins et al., 2008), but could be extended to the new interactions identified by our study. Since JNK has many physiological functions, drugs that target the JIP1 scaffold protein may provide greater selectivity for suppression of JNK activation caused by metabolic stress. Such drugs may be useful for the treatment of obesity-induced metabolic stress, including metabolic syndrome and type 2 diabetes (Kaneto et al., 2004).

EXPERIMENTAL PROCEDURES

Mice

C57BL/6J mice (stock number 000664) and *Rosa-Cre*^{ERT} mice (stock number 00487) (Badea et al., 2003) were obtained from The Jackson Laboratory. We have previously described *Jip1*$^{-/-}$ mice (Whitmarsh et al., 2001), *Mkk7*$^{LoxP/LoxP}$ mice (Hubner et al., 2012), *Mlk2*$^{-/-}$ mice (Kant et al., 2011), *Mlk3*$^{-/-}$ mice (Brancho et al., 2005), *Mlk3*$^{\Delta CRIB/\Delta CRIB}$ mice (Kant et al., 2011), and *Vav1*$^{-/-}$ *Vav2*$^{-/-}$ *Vav3*$^{-/-}$ mice (Fujikawa et al., 2003) on a C57BL/6J strain background.

Mice with a defect in the JNK binding domain of JIP1 (replacement of Leu^{160}-Asn^{161}-Leu^{162} with Gly^{160}-Arg^{161}-Gly^{162}) were established using homologous recombination in embryonic stem (ES) cells using standard methods (Figure S2). The mutated allele was designated *Jip1*$^{\Delta JBD}$. Briefly, a targeting vector was constructed (Figure S2A). This targeting vector was designed to introduce point mutations in exon 3 of the *Jip1* gene that create the ΔJBD mutation and also the introduction of an *Eag*I restriction site (Figure S2A,B). The targeting vector was also designed to introduce a floxed *Neo*^{R} cassette in intron 3 (Figure S2A). TC1 embryonic stem cells (strain 129svev) were electroporated with this vector and selected with 200 μg/ml G418 (Invitrogen) and 2 μM gancyclovir (Syntex). ES cell clones with the floxed *Neo*^{R} cassette correctly inserted in intron 3 were identified by Southern blot analysis (Figure S2C). These ES cells included clones without (genotype *+/Neo*^{R}*-Jip1*^{WT}) and with (genotype *+/Neo*^{R}*-Jip1*$^{\Delta JBD}$) the ΔJBD mutation in exon 3 were identified (Figure S2D). These ES cells were injected into C57BL/6J blastocysts to create chimeric mice that were bred to obtain germ-line transmission of the targeted *Jip1* allele. The floxed *Neo*^{R} cassette was excised using *Cre* recombinase. The mice used in this study were backcrossed (ten generations) to the C57BL/6J strain (Jackson Laboratories).

Male mice (8 – 10 wks. old) were fed a chow diet (Iso Pro 3000, Purina) or a HFD (F3282, Bioserve). Mice were housed in a facility accredited by the American Association for

Laboratory Animal Care. The Institutional Animal Care and Use Committee of the University of Massachusetts Medical School approved all studies using animals.

Genotype analysis

PCR analysis of genomic DNA was employed to detect *Jip1*$^{-}$ (Whitmarsh et al., 2001), *Mlk2*$^{-}$ (Kant et al., 2011), *Mlk3*$^{-}$ (Brancho et al., 2005), *Mlk3*$^{\Delta CRIB}$ (Kant et al., 2011), and *Vav1*$^{-}$, *Vav2*$^{-}$ & *Vav3*$^{-}$ (Fujikawa et al., 2003) alleles. The *Jip1*$^{\Delta JBD}$ allele was detected using three different assays. First, Southern blot analysis of *Hind*III restricted genomic DNA was performed by probing with a 500 base pair fragment of the *Jip1* gene that was isolated by PCR using the primers 5'-CACATCTTGTGTGCTCAATCCG -3' and 5'-GTTCTGGCTTCTGATACTGAACCC - 3'. The *Jip1*$^{+}$ and *Jip1*$^{\Delta JBD}$ alleles were detected as 11.9 kb and 6.6 kb genomic fragments, respectively (Figure S2C). Second, a PCR assay was employed using the primers 5´-GCAAGCTGGGAAGATGACTTTATG-3' and 5'-AGACTGC CTTGGGAAAAGCG-3' and *Eag*I digestion to yield 2.1 kb (*Jip1*$^{+}$) or 1.175 kb plus 0.925 kb DNA fragments (*Jip1*$^{\Delta JBD}$) (Figure S2D). Third, backcrossed mice were genotyped by PCR using the primers 5'-CCAAGTTGTGTGTGGAG AGCTTG-3' and 5'-GCAGATGTTGGAGGAAGAAGC AC-3' to yield a 400 bp DNA fragment (*Jip1*$^{+}$) or a 450 bp DNA fragment (*Jip1*$^{\Delta JBD}$) (Figure S2E).

Plasmids

The retroviral vector pBABE-puro (Morgenstern and Land, 1990) was obtained from Add-gene (plasmid #1764). The *Jip1b* cDNA was modified by insertion of a sequence encoding the T7 epitope tag between codons 1 and 2 (Whitmarsh et al., 1998) and was cloned as a blunt-end fragment into the *Eco*RI site of pBABE-puro. Point mutations in the *Jip1b* cDNA were made using primers 5'-CGACTGAGGAGATCTTCCTGACCCCAGTGC-3' and 5'-GCTGACTCCTCTAGAAGGACTGGGGTCACG-3' (for JIP1b^{Y278F}) and two pairs of primers 5'-CTCTGCCACTGTCTTTGACAACTGTGCCTC-3' plus 5'-GAGACGGTGACAGAAACTGTTGACACGGAG-3' and 5'-GCCATTGGTGAGGAGTTTGA GGAGGCCCCTC-3' plus 5'-CGGTAACCACTCCTCAAACTCCTCCGGGGAG-3' (for JIP1b$^{Y409/427F}$) with a QuikChange II XL kit (Stratagene) and confirmed by DNA sequence analysis. The mammalian expression vectors for SRC (Plasmid #26983) and constitutively active SRC^{Y529F} (Plasmid #17686) were obtained from Add-gene. Bacterial expression vectors for His$_6$-SRC-SH2 and His$_6$-VAV-SH2 (pET28 sacB AP vector with kanamycin resistance) were purchased from OpenBioSytems (#OHS4902_SH2).

Cell culture

Src$^{-/-}$ *Fyn*$^{-/-}$ *Yes*$^{-/-}$ fibroblasts complemented without and with SRC (Klinghoffer et al., 1999) were obtained from the American Type Culture Collection (CRL2459 and CRL2498). RIN5F cells expressing Glu-Glu-tagged JIP1b have been described previously (Standen et al., 2009). Primary WT MEF, *Jip1*$^{-/-}$ MEF, *Jip1*$^{\Delta JBD/\Delta JBD}$ MEF, *Mlk2*$^{-/-}$ *Mlk3*$^{-/-}$ MEF, and *Mlk2*$^{-/-}$ *Mlk3*$^{\Delta CRIB/\Delta CRIB}$ MEF were isolated and cultured *in vitro* (Kant et al., 2011). *Mkk7*$^{-/-}$ MEF were prepared by treating *Rosa-Cre*^{ERT} *Mkk7*$^{LoxP/LoxP}$ MEF with 1μM 4-hydroxytamoxifen (24 h). MEF transduced with pBABE-puro retroviral vectors were selected by incubation (24 h) with 10 μg/ml puromycin (Lamb et al., 2003). Studies of

primary MEF were performed using cells between passages 3 – 5. Cells were transferred to Dulbecco's modified Eagle's Medium supplemented with 0.5% fetal bovine serum (Life Technologies) and incubated (1 h) prior to treatment with 0.5% (w/v) BSA or 0.75 mM palmitate / (w/v) 0.5% BSA. Cells were treated with 1 μM Imatinib (Gleevec) or 10 nM Saracatinib (AZD0530) (Selleck Chemicals). Plasmid transfection assays were performed using Lipofectamine (Life Technologies).

Lipid Raft Isolation

Methods for detergent-dependent lipid raft isolation were described earlier (Holzer et al., 2011; Lingwood and Simons, 2007). Briefly, cells were prepared using Triton lysis buffer [20 mM Tris (pH 7.4), 1% Triton X-100, 10% glycerol, 137 mM NaCl, 2 mM EDTA, 25 mM β-glycerophosphate, 1 mM sodium orthovanadate, 1 mM phenylmethylsulfonyl fluoride, and 10 μg/mL of aprotinin plus leupeptin], sheared with a 25-gauge needle and incubated at 4°C (30 min). Optiprep (Sigma) 40%–30%-5% step gradients were prepared prior to flotation of the cell lysate on the step gradient, and centrifugation (16 hr at 260000 × *g*). Raft and non-raft fractions were collected and examined by protein immunoblot analysis.

Immunoblot analysis

Cell extracts were prepared using Triton lysis buffer (20mM Tris (pH 7.4), 1% Triton X-100, 10% glycerol, 137 mM NaCl, 2 mM EDTA, 25 mM β-glycerophosphate, 1 mM sodium orthovanadate, 1 mM phenylmethylsulfonyl fluoride, 10 μg/mL aprotinin and leupeptin) for 20 minutes at ice. Triton soluble and insoluble fractions were prepared by centrifugation at 13,000 rpm (10 min) and examined by protein immunoblot analysis. Primary antibodies were obtained from Cell Signaling (MLK3, pJNK, SRC & pY^{416}-SRC), Covance (Glu-Glu tag), Life Technologies (JNK, Flotillin1 & JIP1), Millipore (T7 tag), Santa Cruz Biotechnologies (VAV2, Flotillin2), and Sigma (αTubulin). Immunecomplexes were detected by enhanced chemiluminescence (New England Nuclear) using an ImageQuant LAS4000 (General Electric).

Immunoprecipitation

Cell extracts were prepared using NP40 lysis buffer (150 mM NaCl, 50 mM Tris (pH 8.0), 5 mM EDTA, 1% NP-40, 1 mM sodium orthovanadate, 1 mM phenylmethylsulfonyl fluoride, 10 mg/mL aprotinin and leupeptin) and incubated (5 h at 4°C) with 10 μg of control nonimmune rabbit IgG (Santa Cruz Biotechnologies) or 10 μg of rabbit antibodies to the Glu-Glu tag (Covance) or JIP1 (Yasuda et al., 1999). Immunecomplexes isolated using Protein G Sepharose (Sigma) were washed (five times) with lysis buffer.

In vitro SH2 domain interaction assays

Bacterial expression of His_6-SRC-SH2 and His_6-VAV-SH2 was induced with 1mM IPTG (3 h, 37°C). The bacteria were lysed by sonication in Buf fer X (20mMTris at pH 7.4, 1M NaCl, 0.2 mM EDTA, 0.2 mM EGTA, 1mM DTT, 1 mM phenylmethylsulfonyl fluoride, 10 μg/mL aprotinin and leupeptin). The soluble extract was clarified by centrifugation. The supernatant was incubated (1 h at 4°C) with 20 μL nickel magnetic beads (GE Heal thcare Life Sciences # 28-9781-19 AB). The beads were washed with Buffer X and then incubated

with extracts (100 μg protein) prepared from WT and *Jip1*$^{-/-}$ MEF using Triton lysis buffer (20 mM Tris (pH 7.4), 1% Triton X-100, 10% glycerol, 137 mM NaCl, 2 mM EDTA, 25 mM β-glycerophosphate, 1 mM sodium orthovanadate, 1 mM phenylmethylsulfonyl fluoride, 10 μg/mL of aprotinin and leupeptin). The beads were washed with Triton lysis buffer and bound proteins were examined by immunoblot analysis.

Immunofluorescence

Cells grown on glass coverslips were treated (1 min) at room temperature (RT) with 0.5% Triton X-100 in phosphate-buffered saline (PBS) and then fixed by incubation at 4°C in 4% paraformaldehyde (30 min). The coverslips were incubated (1 h) with blocking buffer (3% (w/v) BSA in PBS) at room temperature (RT), and then incubated (1 h) with primary antibodies diluted in blocking buffer at RT. The primary antibodies to the Glu-Glu epitope tag (Covance) and SRC (Cell Signaling) were used. The coverslips were washed with 0.5% Tween 20 / PBS. The primary antibodies were detected by incubation with anti-mouse or anti-rabbit immunoglobulin conjugated to Alexa Fluor 488 or 546 (Life Technologies). Fluorescence was visualized using a Leica TCS SP2 confocal microscope equipped with a 405-nm diode laser.

Supplementary Material

Refer to Web version on PubMed Central for supplementary material.

Acknowledgments

We thank Vicky Benoit and Heather Learnard for expert technical assistance, and Kathy Gemme for administrative assistance. These studies were supported by National Institutes of Health grants DK107220 and DK112698 (to RJD) and American Heart Association grant 16SDG29660007 (to SK). The UMASS Mouse Metabolic Phenotyping Center is supported by National Institutes of Health grant DK093000 (to JK). RAF and RJD are Investigators of the Howard Hughes Medical Institute.

References

Alvarez-Curto E, Milligan G. Metabolism meets immunity: The role of free fatty acid receptors in the immune system. Biochem Pharmacol. 2016

Badea TC, Wang Y, Nathans J. A noninvasive genetic/pharmacologic strategy for visualizing cell morphology and clonal relationships in the mouse. J Neurosci. 2003; 23:2314–2322. [PubMed: 12657690]

Brancho D, Ventura JJ, Jaeschke A, Doran B, Flavell RA, Davis RJ. Role of MLK3 in the regulation of mitogen-activated protein kinase signaling cascades. Mol Cell Biol. 2005; 25:3670–3681. [PubMed: 15831472]

Chen T, Kablaoui N, Little J, Timofeevski S, Tschantz WR, Chen P, Feng J, Charlton M, Stanton R, Bauer P. Identification of small-molecule inhibitors of the JIP-JNK interaction. Biochem J. 2009; 420:283–294. [PubMed: 19243309]

Craige SM, Reif MM, Kant S. Mixed - Lineage Protein kinases (MLKs) in inflammation, metabolism, and other disease states. Biochim Biophys Acta. 2016; 1862:1581–1586. [PubMed: 27259981]

Crespo P, Bustelo XR, Aaronson DS, Coso OA, Lopez-Barahona M, Barbacid M, Gutkind JS. Rac-1 dependent stimulation of the JNK/SAPK signaling pathway by Vav. Oncogene. 1996; 13:455–460. [PubMed: 8760286]

Crespo P, Schuebel KE, Ostrom AA, Gutkind JS, Bustelo XR. Phosphotyrosine-dependent activation of Rac-1 GDP/GTP exchange by the vav protooncogene product. Nature. 1997; 385:169–172. [PubMed: 8990121]

D'Ambrosio C, Arena S, Fulcoli G, Scheinfeld MH, Zhou D, D'Adamio L, Scaloni A. Hyperphosphorylation of JNK-interacting protein 1, a protein associated with Alzheimer disease. Mol Cell Proteomics. 2006; 5:97–113. [PubMed: 16195223]

Dajas-Bailador F, Jones EV, Whitmarsh AJ. The JIP1 scaffold protein regulates axonal development in cortical neurons. Curr Biol. 2008; 18:221–226. [PubMed: 18261906]

Davis RJ. MAPKs: new JNK expands the group. Trends Biochem Sci. 1994; 19:470–473. [PubMed: 7855889]

Davis RJ. Signal transduction by the JNK group of MAP kinases. Cell. 2000; 103:239–252. [PubMed: 11057897]

Flegal KM, Kit BK, Orpana H, Graubard BI. Association of all-cause mortality with overweight and obesity using standard body mass index categories: a systematic review and meta-analysis. JAMA. 2013; 309:71–82. [PubMed: 23280227]

Fu S, Watkins SM, Hotamisligil GS. The role of endoplasmic reticulum in hepatic lipid homeostasis and stress signaling. Cell Metab. 2012; 15:623–634. [PubMed: 22560215]

Fujikawa K, Miletic AV, Alt FW, Faccio R, Brown T, Hoog J, Fredericks J, Nishi S, Mildiner S, Moores SL, et al. Vav1/2/3-null mice define an essential role for Vav family proteins in lymphocyte development and activation but a differential requirement in MAPK signaling in T and B cells. J Exp Med. 2003; 198:1595–1608. [PubMed: 14623913]

Heo YS, Kim SK, Seo CI, Kim YK, Sung BJ, Lee HS, Lee JI, Park SY, Kim JH, Hwang KY, et al. Structural basis for the selective inhibition of JNK1 by the scaffolding protein JIP1 and SP600125. EMBO J. 2004; 23:2185–2195. [PubMed: 15141161]

Hernandez ED, Lee SJ, Kim JY, Duran A, Linares JF, Yajima T, Muller TD, Tschop MH, Smith SR, Diaz-Meco MT, et al. A macrophage NBR1-MEKK3 complex triggers JNK-mediated adipose tissue inflammation in obesity. Cell Metab. 2014; 20:499–511. [PubMed: 25043814]

Holzer RG, Park EJ, Li N, Tran H, Chen M, Choi C, Solinas G, Karin M. Saturated fatty acids induce c-Src clustering within membrane subdomains, leading to JNK activation. Cell. 2011; 147:173–184. [PubMed: 21962514]

Hu W, Bielawski J, Samad F, Merrill AH Jr, Cowart LA. Palmitate increases sphingosine-1-phosphate in C2C12 myotubes via upregulation of sphingosine kinase message and activity. J Lipid Res. 2009; 50:1852–1862. [PubMed: 19369694]

Hubner A, Mulholland DJ, Standen CL, Karasarides M, Cavanagh-Kyros J, Barrett T, Chi H, Greiner DL, Tournier C, Sawyers CL, et al. JNK and PTEN cooperatively control the development of invasive adenocarcinoma of the prostate. Proc Natl Acad Sci U S A. 2012; 109:12046–12051. [PubMed: 22753496]

Jaeschke A, Czech MP, Davis RJ. An essential role of the JIP1 scaffold protein for JNK activation in adipose tissue. Genes Dev. 2004; 18:1976–1980. [PubMed: 15314024]

Jaeschke A, Davis RJ. Metabolic stress signaling mediated by mixed-lineage kinases. Mol Cell. 2007; 27:498–508. [PubMed: 17679097]

Kahn SE, Hull RL, Utzschneider KM. Mechanisms linking obesity to insulin resistance and type 2 diabetes. Nature. 2006; 444:840–846. [PubMed: 17167471]

Kaneto H, Nakatani Y, Miyatsuka T, Kawamori D, Matsuoka TA, Matsuhisa M, Kajimoto Y, Ichijo H, Yamasaki Y, Hori M. Possible novel therapy for diabetes with cell-permeable JNK-inhibitory peptide. Nat Med. 2004; 10:1128–1132. [PubMed: 15448687]

Kant S, Barrett T, Vertii A, Noh YH, Jung DY, Kim JK, Davis RJ. Role of the mixed-lineage protein kinase pathway in the metabolic stress response to obesity. Cell Rep. 2013; 4:681–688. [PubMed: 23954791]

Kant S, Swat W, Zhang S, Zhang ZY, Neel BG, Flavell RA, Davis RJ. TNF-stimulated MAP kinase activation mediated by a Rho family GTPase signaling pathway. Genes Dev. 2011; 25:2069–2078. [PubMed: 21979919]

Kennedy NJ, Martin G, Ehrhardt AG, Cavanagh-Kyros J, Kuan CY, Rakic P, Flavell RA, Treistman SN, Davis RJ. Requirement of JIP scaffold proteins for NMDA-mediated signal transduction. Genes Dev. 2007; 21:2336–2346. [PubMed: 17875667]

Klinghoffer RA, Sachsenmaier C, Cooper JA, Soriano P. Src family kinases are required for integrin but not PDGFR signal transduction. EMBO J. 1999; 18:2459–2471. [PubMed: 10228160]

Lamb JA, Ventura JJ, Hess P, Flavell RA, Davis RJ. JunD mediates survival signaling by the JNK signal transduction pathway. Mol Cell. 2003; 11:1479–1489. [PubMed: 12820962]

Lingwood D, Simons K. Detergent resistance as a tool in membrane research. Nat Protoc. 2007; 2:2159–2165. [PubMed: 17853872]

Montell E, Turini M, Marotta M, Roberts M, Noe V, Ciudad CJ, Mace K, Gomez-Foix AM. DAG accumulation from saturated fatty acids desensitizes insulin stimulation of glucose uptake in muscle cells. Am J Physiol Endocrinol Metab. 2001; 280:E229–237. [PubMed: 11158925]

Moran BM, Flatt PR, McKillop AM. G protein-coupled receptors: signalling and regulation by lipid agonists for improved glucose homoeostasis. Acta Diabetol. 2016

Morel C, Standen CL, Jung DY, Gray S, Ong H, Flavell RA, Kim JK, Davis RJ. Requirement of JIP1-mediated c-Jun N-terminal kinase activation for obesity-induced insulin resistance. Mol Cell Biol. 2010; 30:4616–4625. [PubMed: 20679483]

Morgenstern JP, Land H. Advanced mammalian gene transfer: high titre retroviral vectors with multiple drug selection markers and a complementary helper-free packaging cell line. Nucleic Acids Res. 1990; 18:3587–3596. [PubMed: 2194165]

Neuschwander-Tetri BA. Hepatic lipotoxicity and the pathogenesis of nonalcoholic steatohepatitis: the central role of nontriglyceride fatty acid metabolites. Hepatology. 2010; 52:774–788. [PubMed: 20683968]

Nihalani D, Wong H, Verma R, Holzman LB. Src family kinases directly regulate JIP1 module dynamics and activation. Mol Cell Biol. 2007; 27:2431–2441. [PubMed: 17242197]

Sabio G, Davis RJ. cJun NH2-terminal kinase 1 (JNK1): roles in metabolic regulation of insulin resistance. Trends Biochem Sci. 2010; 35:490–496. [PubMed: 20452774]

Schmitz-Peiffer C, Craig DL, Biden TJ. Ceramide generation is sufficient to account for the inhibition of the insulin-stimulated PKB pathway in C2C12 skeletal muscle cells pretreated with palmitate. J Biol Chem. 1999; 274:24202–24210. [PubMed: 10446195]

Sharma M, Urano F, Jaeschke A. Cdc42 and Rac1 are major contributors to the saturated fatty acid-stimulated JNK pathway in hepatocytes. J Hepatol. 2012; 56:192–198. [PubMed: 21703174]

Songyang Z, Shoelson SE, Chaudhuri M, Gish G, Pawson T, Haser WG, King F, Roberts T, Ratnofsky S, Lechleider RJ, et al. SH2 domains recognize specific phosphopeptide sequences. Cell. 1993; 72:767–778. [PubMed: 7680959]

Songyang Z, Shoelson SE, McGlade J, Olivier P, Pawson T, Bustelo XR, Barbacid M, Sabe H, Hanafusa H, Yi T, et al. Specific motifs recognized by the SH2 domains of Csk, 3BP2, fps/fes, GRB-2, HCP, SHC, Syk, and Vav. Mol. Cell. Biol. 1994; 14:2777–2785. [PubMed: 7511210]

Standen CL, Kennedy NJ, Flavell RA, Davis RJ. Signal transduction cross talk mediated by Jun N-terminal kinase-interacting protein and insulin receptor substrate scaffold protein complexes. Mol Cell Biol. 2009; 29:4831–4840. [PubMed: 19564410]

Stebbins JL, De SK, Machleidt T, Becattini B, Vazquez J, Kuntzen C, Chen LH, Cellitti JF, Riel-Mehan M, Emdadi A, et al. Identification of a new JNK inhibitor targeting the JNK-JIP interaction site. Proc Natl Acad Sci U S A. 2008; 105:16809–16813. [PubMed: 18922779]

Teramoto H, Coso OA, Miyata H, Igishi T, Miki T, Gutkind JS. Signaling from the small GTP-binding proteins Rac1 and Cdc42 to the c-Jun N-terminal kinase/stress-activated protein kinase pathway. A role for mixed lineage kinase 3/protein-tyrosine kinase 1, a novel member of the mixed lineage kinase family. J Biol Chem. 1996; 271:27225–27228. [PubMed: 8910292]

Whitmarsh AJ, Cavanagh J, Tournier C, Yasuda J, Davis RJ. A mammalian scaffold complex that selectively mediates MAP kinase activation. Science. 1998; 281:1671–1674. [PubMed: 9733513]

Whitmarsh AJ, Kuan CY, Kennedy NJ, Kelkar N, Haydar TF, Mordes JP, Appel M, Rossini AA, Jones SN, Flavell RA, et al. Requirement of the JIP1 scaffold protein for stress-induced JNK activation. Genes Dev. 2001; 15:2421–2432. [PubMed: 11562351]

Yasuda J, Whitmarsh AJ, Cavanagh J, Sharma M, Davis RJ. The JIP group of mitogen-activated protein kinase scaffold proteins. Mol Cell Biol. 1999; 19:7245–7254. [PubMed: 10490659]

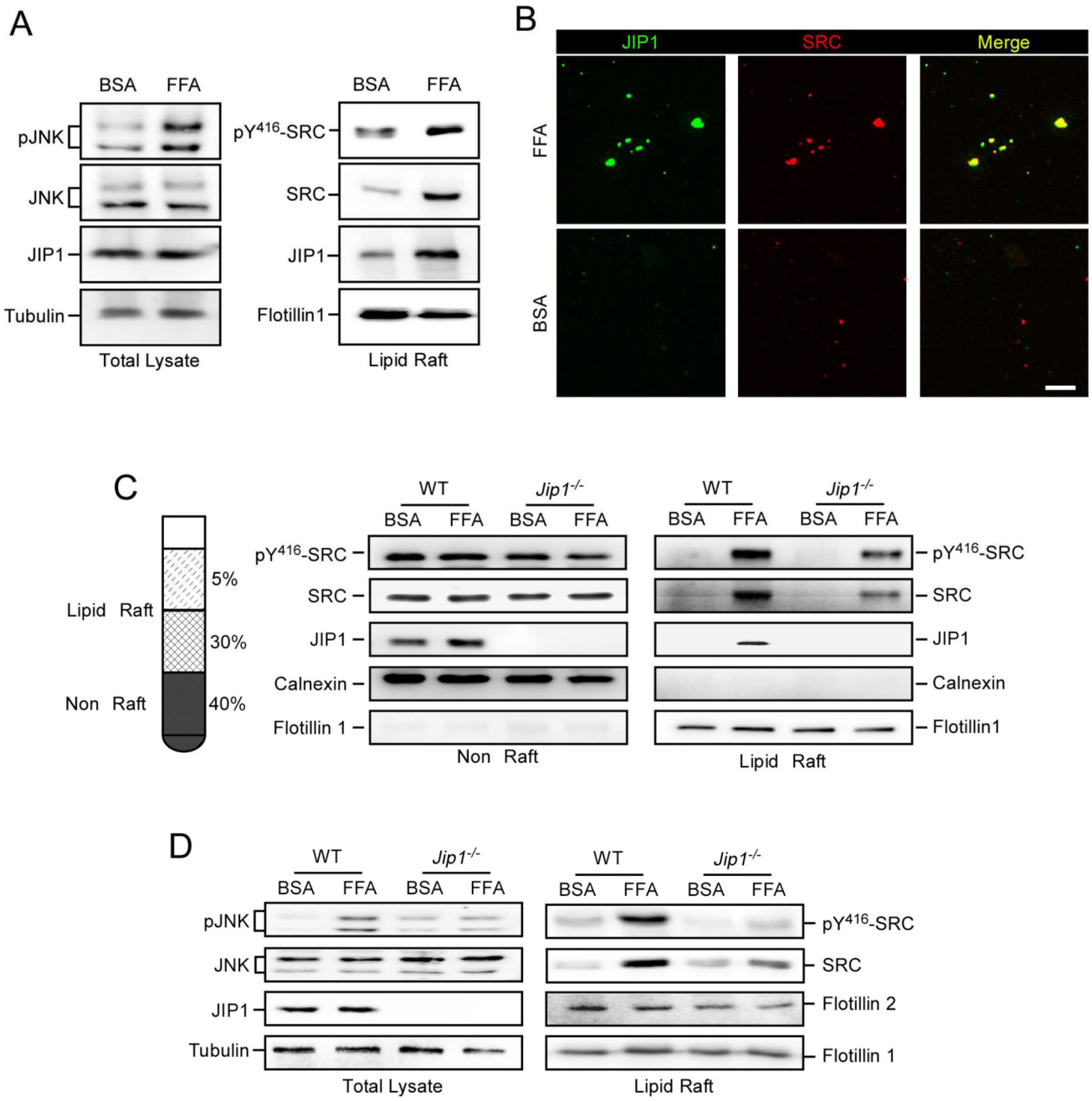

Figure 1. JIP1 is required for palmitate-induced localization of SRC to lipid rafts

(**A,B**) RIN5F cells expressing EE-tagged JIP1 were treated (4 h) with fatty acid-free bovine serum albumin (BSA) or palmitate/BSA (FFA). The total cell lysate and the Triton insoluble lipid raft fraction were examined by immunoblot analysis (A). Cells permeabilized with Triton X-100 and fixed were examined by immunofluorescence analysis (B). Scale bar = 10 μm.

(**C,D**) WT and *Jip1*$^{-/-}$ MEF were treated (4 h) with BSA or FFA. An Optiprep 40%–30%-5% step gradient separated raft and non-raft fractions for examination by immunoblot

analysis (C). The total cell lysate and the Triton insoluble lipid raft fraction were examined by immunoblot analysis (D).
See also Figure S1.

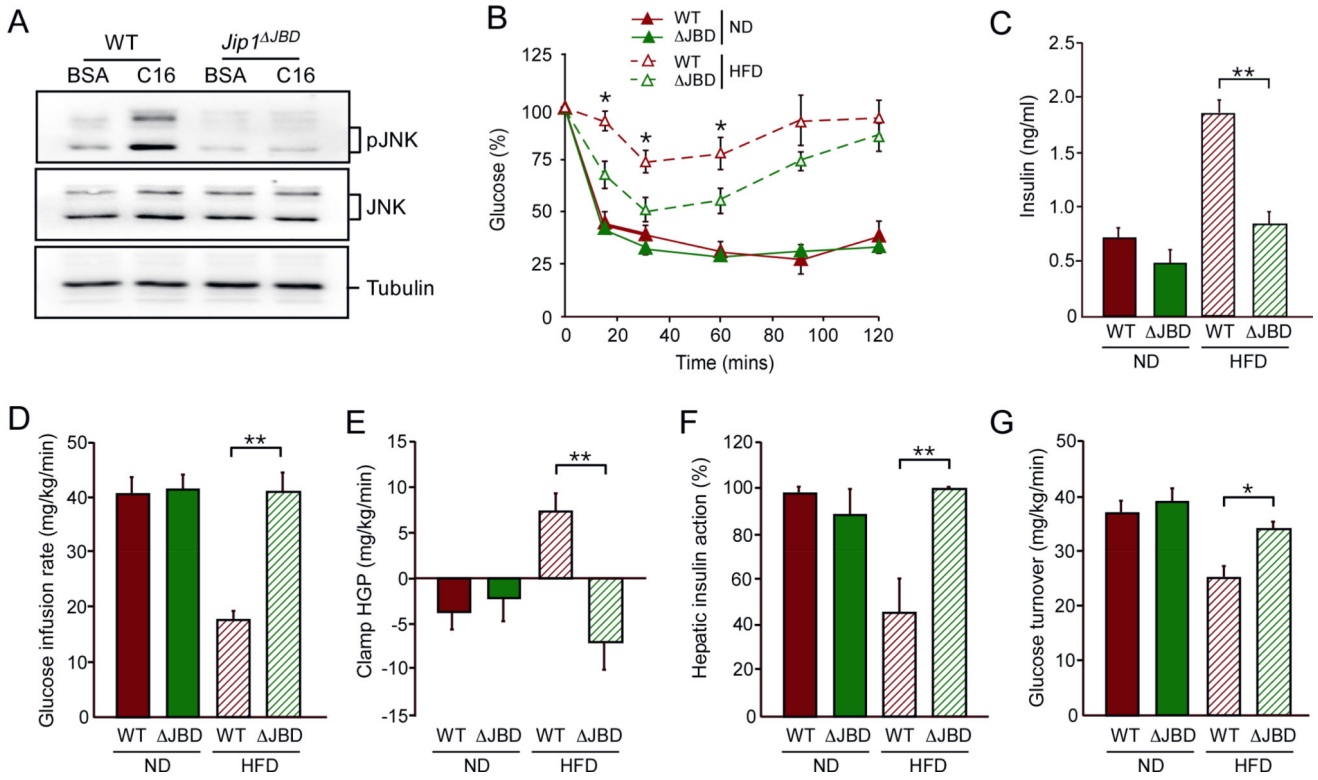

Figure 2. JIP1-mediated JNK activation promotes HFD-induced insulin resistance

(**A**) Control (BSA) and palmitate (FFA)-stimulated (16 h) WT and JNK$^{\Delta JDB}$ MEF were examined by immunoblot analysis.

(**B**) WT and JNK$^{\Delta JDB}$ mice were fed a chow diet (ND) or a HFD (16 wk) and examined with an insulin tolerance test. The time course of insulin-stimulated glucose clearance is presented (mean ± SEM; n = 10; *, $p < 0.05$).

(**C**) The blood concentration of insulin was measured by ELISA (mean ± SEM; n = 10; **, $p < 0.01$).

(**D–G**) The glucose infusion rate (D), clamp hepatic glucose production (E), hepatic insulin action (F), and whole body glucose turnover (G) measured by hyperinsulinemic-euglycemic clamp analysis (mean ± SEM; n = 8; *, $p < 0.05$; **, $p < 0.01$).

See also Figure S2–S4.

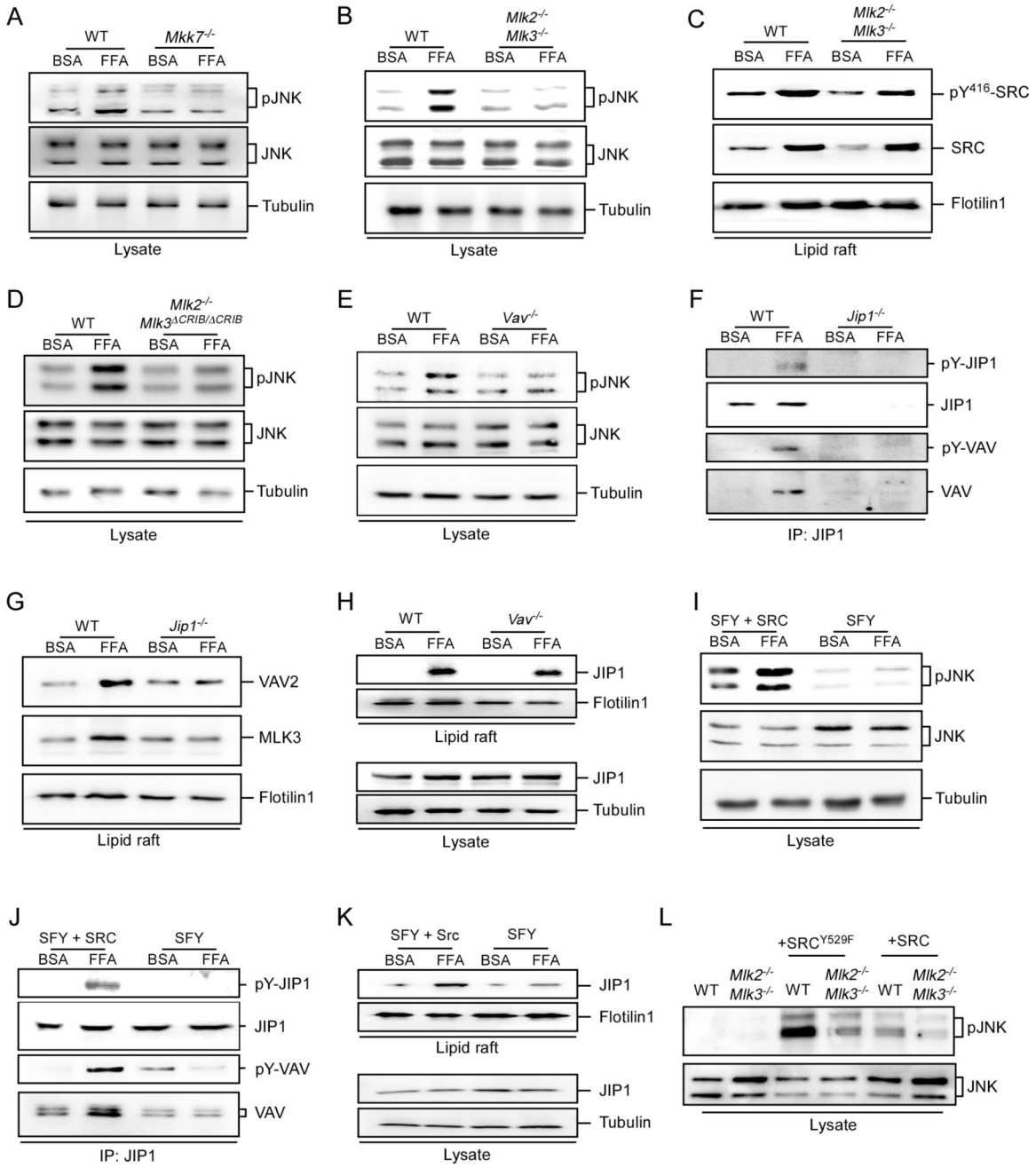

Figure 3. VAV, RAC1, MLK, and MKK7 contribute to JIP1-mediated JNK activation

(**A,B**) WT and *Mkk7*$^{-/-}$ MEF (A) or *Mlk2*$^{-/-}$ *Mlk3*$^{-/-}$ MEF (B) were treated (16 h) without (BSA) or with palmitate/BSA (FFA) and subsequently examined by immunoblot analysis.

(**C**) The lipid raft fraction of WT and *Mlk2*$^{-/-}$ *Mlk3*$^{-/-}$ MEF treated (4 h) without (BSA) or with palmitate/BSA (FFA) was examined by immunoblot analysis.

(**D**) WT and *Mlk2*$^{-/-}$ *Mlk*$^{-\Delta CRIB/\Delta CRIB}$ MEF were treated with BSA or FFA/BSA (16 h) and examined by immunoblot analysis.

(**E**) WT and *Vav1*$^{-/-}$ *Vav2*$^{-/-}$ *Vav3*$^{-/-}$ (*Vav*$^{-/-}$) cells were treated with BSA or FFA/BSA (16 h) and examined by immunoblot analysis.

(**F,G**) WT and *Jip1*$^{-/-}$ MEF were treated with BSA or FFA. JIP1 immunoprecipitates (F) and isolated lipid rafts (G) were examined by immunoblot analysis.
(**H**) WT and *Vav1*$^{-/-}$ *Vav2*$^{-/-}$ *Vav3*$^{-/-}$ (*Vav*$^{-/-}$) cells were transduced with a retrovirus expressing EE-tagged JIP1. The cells were treated with BSA or FFA/BSA (4 h) and examined by immunoblot analysis of cell lysates and isolated lipid rafts.
(**I–K**) *Src*$^{-/-}$ *Fyn*$^{-/-}$ *Yes*$^{-/-}$ (SFY) fibroblasts and SFY cells complemented with SRC (SFY + SRC) fibroblasts were transduced with a retrovirus expressing EE-tagged JIP1. The cells were treated with BSA or FFA/BSA and examined by immunoblot analysis of cell lysate (I), JIP1 immunoprecipitates (J), or isolated lipid rafts (K).
(**L**) Constitutively activated SRC (SRC^{Y529F}) and SRC expression plasmids were employed in transfection assays with WT and *Mlk2*$^{-/-}$ *Mlk3*$^{-/-}$ MEF. Cell lysates were prepared at 24 h post-transfection and examined by immunoblot analysis.

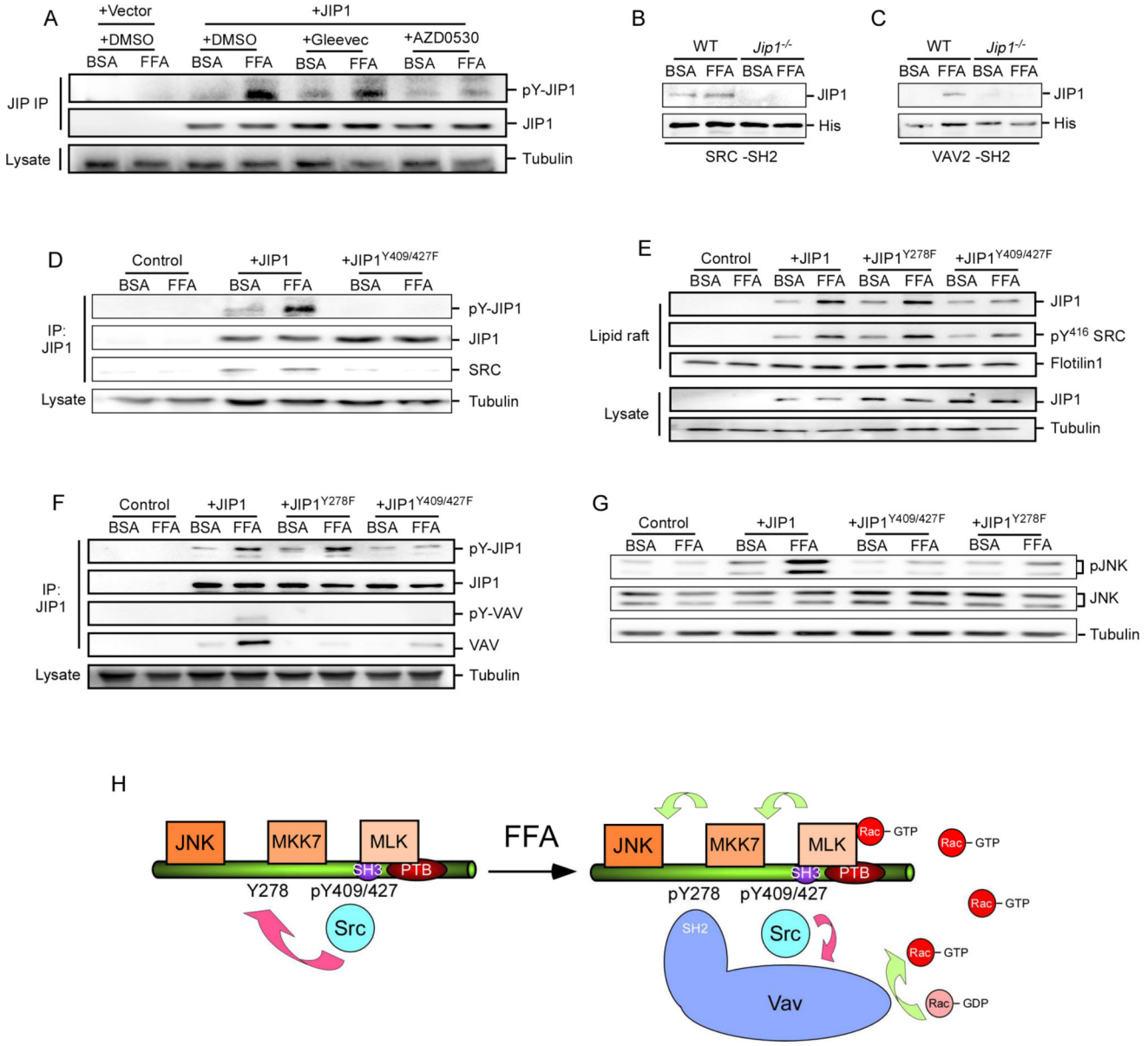

Figure 4. Tyrosine phosphorylation of JIP1 is necessary for palmitate-induced tethering of SRC / VAV and JNK activation

(**A**) *Jip1*$^{-/-}$ MEF were transduced with an empty retroviral vector (Control) or with a retroviral vector that expresses T7-tagged JIP1. The MEF were treated with or without Gleevec (1μM) or AZD0530 (10nM) for 30 minutes before addition of BSA or FFA/BSA (4 h). Cell lysates and JIP1 immunoprecipitates were examined by immunoblot analysis. (**B,C**) His_6-SRC-SH2 and His_6-VAV2-SH2 immobilized on nickel beads were incubated with extracts prepared from WT and *Jip1*$^{-/-}$ MEF treated with BSA or FFA (4 h). Bound proteins were detected by immunoblot analysis using antibodies to His_6 and JIP1. (**D–F**) *Jip1*$^{-/-}$ MEF were transduced with an empty retroviral vector (Control) or with a retroviral vector that expresses T7-tagged JIP1, JIP1^{Y278F}, or JIP1$^{Y409/427F}$. The MEF were

treated with BSA or FFA/BSA (4 h). Cell lysates, isolated lipid rafts, and JIP1 immunoprecipitates were examined by immunoblot analysis.

(**G**) *Jip1*$^{-/-}$ MEF (Control) and *Jip1*$^{-/-}$ MEF expressing T7-tagged JIP1, JIP1^{Y278F}, or JIP1$^{Y409/427F}$ were treated with BSA or FFA/BSA (16 h) and cell lysates were examined by immunoblot analysis.

(**H**) Schematic illustration of JIP1-mediated activation in response to exposure to FFA.